Airport multipath simulation and measurement tool for siting DGPS reference stations

Christophe Macabiau, Benoit Roturier, Eric Chatre, Alain Renard

AIRPORT MULTIPATH SIMULATION AND MEASUREMENT TOOL FOR SITING DGPS REFERENCE STATIONS

Christophe MACABIAU, Benoît ROTURIER
CNS Research Laboratory of the ENAC,
ENAC, 7 avenue Edouard Belin, BP 4005, 31055 TOULOUSE CEDEX 4, France
macabiau@recherche.enac.fr
Eric CHATRE, *STNA*
ALAIN RENARD, *SEXTANT AVIONIQUE*

ABSTRACT

The CNS Research Laboratory (URE-CNS) of the ENAC, in collaboration with the STNA and SEXTANT AVIONIQUE, is developing a tool for providing DGPS reference stations siting guidelines for the French Civil Aviation Authority. This tool is based on computed error predictions using mathematical models, and on signal disturbance measurements made at pre-selected locations. The aim of the proposed paper is to present the complete siting tool which was developed along with some examples of its use showing the extent of the validity of its predictions.

I. INTRODUCTION

The siting of a GPS reference station on an airport is achieved by minimizing the influence of the environment on the pseudorange measurements, while complying with the practical operational installation constraints. The CNS Research Laboratory (URE-CNS) of the ENAC, in collaboration with the STNA and SEXTANT AVIONIQUE, has started a study that aims at providing siting guidelines for the French Civil Aviation Authority [Macabiau et al., 1998].

As a result, a tool is developed, based on computed error predictions using mathematical models, and on signal disturbance measurements made at pre-selected locations. The first part of this tool is an end-to-end GPS simulator that is used to establish the main basic rules for the choice of the best configuration and location of the station on an airport with regards to multipath effects by providing analysis of the measurement errors induced by simple obstacles [Macabiau et al., 1999]. The second part of this tool is software designed to extract the measurement errors from the observations made by a GPS receiver connected to an antenna placed at the surveyed location.

The aim of this paper is to present the complete siting tool which was developed along with some examples of its application.

II. DESCRIPTION OF THE SITING TOOL

The simulator is comprised of three cascaded modules, as illustrated in figure 1. The first module computes the position of the satellites with a time step larger than the time of coherence of the propagation channel. The second module simulates the propagation channel. It is derived from the ray-tracing MUSICA tool (MUltipath SImulation for Civil Aviation) that was previously developed by the ENAC for classical navaids multipath simulation. Using the channel transfer function determined through the Uniform Theory of Diffraction, it generates the disturbed signal delivered by the antenna of the station to its receiver front-end. Then, this signal is handed to the last module, that simulates a generic GPS receiver and delivers the range measurement errors induced by the perturbations introduced in the whole propagation channel. It has the ability to predict the influence of reflecting and diffracting objects, such as the ground and buildings on the code and phase measurement errors.

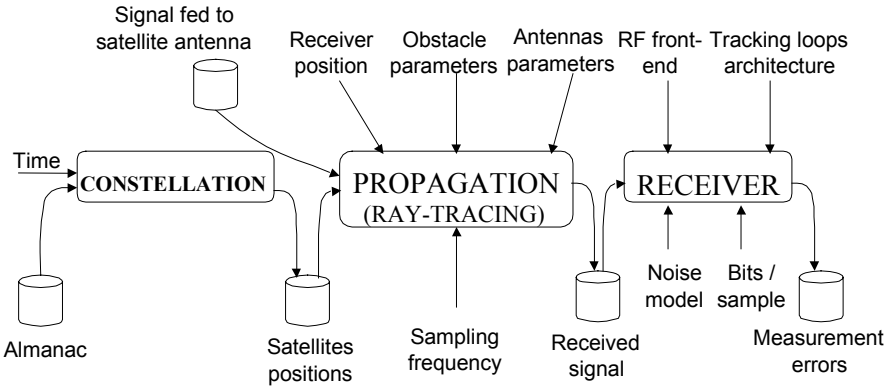

Figure 1: *Architecture of the end-to-end GPS simulator.*

The measuring tool uses the raw data collected by a dual frequency GPS receiver to isolate the measurement errors made by the code tracking loop caused by multipath. The technique consists in forming a multipath observable by summing the code and phase measurements. This multipath observable contains the code and phase tracking errors due to multipath and noise, and is not affected by the satellite-user range variation, as well as the common errors such as tropospheric delay and satellite clock offset, including SA [Braasch, 1996].

The ionospheric divergence contained in the multipath observable is removed by subtracting an estimate of the ionospheric delay formed using the L1 and L2 carrier phase pseudorange measurements, as suggested in [Braasch, 1994]. As the carrier phase observations are less susceptible to multipath, this estimate of the ionospheric delay is less affected by multipath than the classical estimate computed using the code pseudorange measurements. However, this estimate is biased because the carrier phase measurements have an intrinsic ambiguity. This has no importance because the multipath observable is biased by the L1 carrier phase measurement ambiguity anyway.

Once the ionospheric divergence is removed, only remains the code and phase tracking errors due to noise and multipath plus the bias contained in the ionospheric delay estimate and the L1 carrier phase measurement. Assuming the phase tracking errors are negligible compared to their code counterparts, the remaining quantities are the code tracking tracking error due to noise and multipath plus a bias. Note that the bias is removed by subtracting the mean value of this quantity over a given interval. This operation also removes the average value of the multipath error, only leaving the non-zero frequency components. Moreover, as carrier phase measurements are intensively used in this technique, the resulting quantity is highly affected by cycle slips.

The code measurements used by the measuring tool are smoothed using the L1 carrier phase measurements with a 2s smoothing filter. This reduces the noise level, while keeping most of the multipath frequency components, as the antenna is fixed on the ground.

Therefore, the code tracking errors can be isolated from this quantity provided that the PLL and the DLL maintain continuous tracking. Besides any other obvious condition, this is true if the multipath is not too severe to cause a PLL or DLL loss of lock.

III. EXAMPLES

The simulator has undergone a theoretical and a practical validation to check the validity of its predictions.

The theoretical validation has consisted in comparing the predicted code and phase tracking errors in simple artificial well-known situations, involving only one reflector (ground or building

wall), with the theoretical tracking errors. This first validation allowed to correct a few bugs in the software, and the final results showed no failure of the simulator.

The practical validation consists in comparing the predicted code tracking errors in simple situations with the observed real tracking errors in the same situations. The parameters provided to the simulator where chosen to reflect the real situation as closely as we could. The position and height of the antenna on the ground and its distance with respect to the obstacles was measured and inserted in the propagation module. The digitized RHC and LHC patterns of the antennas used for the measurements were fed to the propagation module. The receiver parameters, such as the RF front-end filter bandwidth and the global tracking loop parameters were inserted in the receiver simulation module.

Several sets of measurements were collected in various situations involving different types of obstacles. We present here some results of comparison of measurements and simulation when the main obstacles are the ground and one building.

The first set of measurements presented in this paper was collected on the site of the Toulouse-Blagnac airport DGPS reference station, in a direction where the main reflector is assumed to be only the ground. Figures 2, 3, 4 and 5 show the observed and the simulated values obtained using a choke ring antenna placed 6.6 meters above the ground.

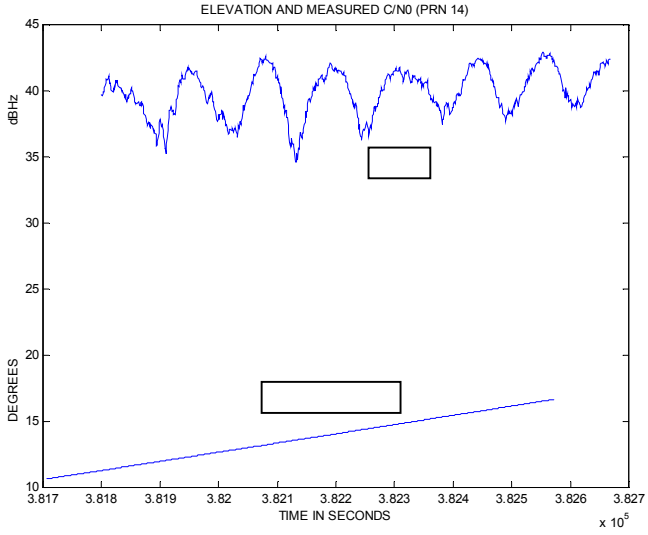

Figure 2: *Measured C/N0 for a choke ring antenna 6.6 m above the ground (PRN 14).*

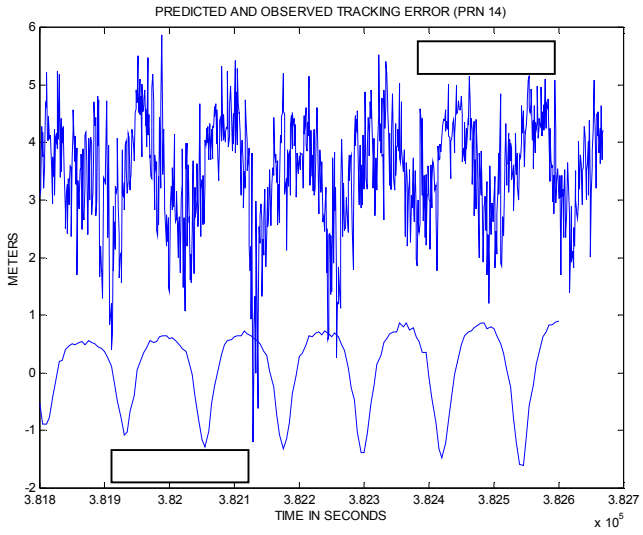

Figure 3: *Comparison of predicted and observed code tracking error for a choke ring antenna 6.6 m above the ground (PRN 14).*

Figure 2 shows the elevation and the measured C/N_0 for PRN 14. As we can see for this rising satellite, the long term evolution of the measured C/N_0 shows that the incoming signal is affected by one reflected signal. But we can also see that faster variations exist, indicating the presence of other diffracted rays.

The upper part of figure 3 shows the extracted code measurement error due to noise and multipath obtained using the technique presented in section II. The error has a high frequency component due to the noise that has a meter level amplitude on this plot. The error has also a low frequency component that can be attributed to multipath. The amplitude of this component is approximately 2 meters, and its period is about 110 s. This period is characteristic of the time required for the ray reflected by the Earth's surface to rotate by one complete L1 wavelength with respect to the direct signal at the antenna phase center located approximately at 6.6 m above the ground.

The lower part of figure 3 shows the predicted tracking error obtained using the simulator. The only obstacle inserted in the simulator is the Earth's surface modeled as a metallic plate. As we can see, the period and the amplitude of the predicted error are compatible with the observed values. The only difference is a phase shift that can be explained by the difficulty to set the dielectric parameters of the soil at this time, and the uncertainty in the height of the antenna above the reflecting ground plane. But this phase shift is not important in this application as the objective is to predict as accurately as possible the shape and the amplitude of the tracking error due to multipath.

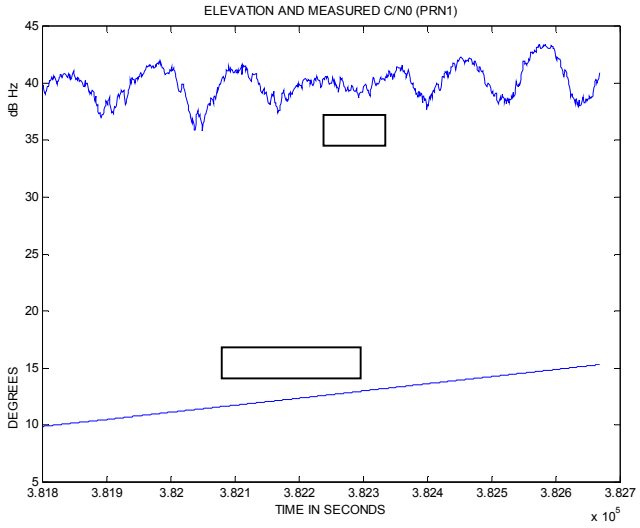

Figure 4: *Measured C/N0 for a choke ring antenna 6.6 m above the ground (PRN 1).*

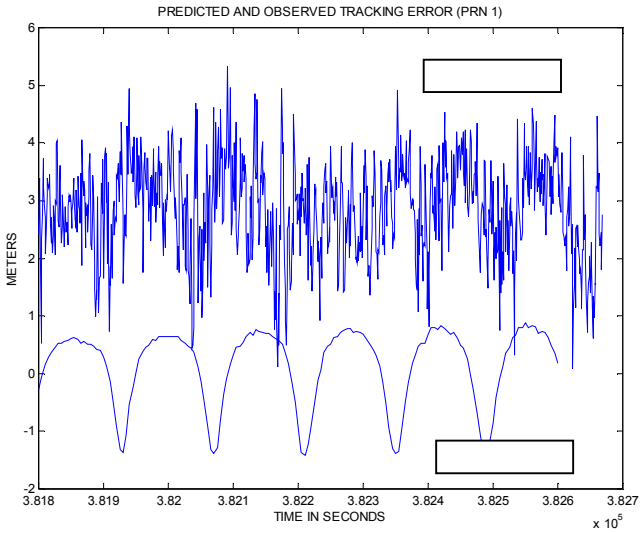

Figure 5: *Comparison of predicted and observed code tracking error for a choke ring antenna 6.6 m above the ground (PRN 1).*

Figure 4 shows the elevation and the measured C/N_0 for PRN 1. Comparing this figure with figure 2 shows that the signal is mainly affected by one reflected ray, but another phenomenon disturbs the signal in the middle of the time interval This could be due to another reflected ray coming from another obstacle, or to a change in the ray reflected by the ground at this point.

The upper curve of figure 5 shows the observed tracking error extracted using the technique presented in section II. As we can see, this curve is highly similar to the curve presented in figure 3, with the exception of the middle interval of the plot.

The lower part of figure 5 shows the predicted code tracking error obtained using the simulator. As we can see, the predicted error corresponds to the long term variation of the curve with the exception that the flatness of the observed error in the middle of the time interval is not reproduced. This deviation between the observed and predicted errors is due to the fact that all the obstacles were not accurately modeled in the simulator. In particular, the DGPS reference station shelter was not modeled in this particular trial.

The second set of measurements presented here was collected on the ENAC campus, and involves one building and the ground. The antenna is a classical patch GPS antenna placed 2.15 m above the ground and 5.5 m away from a building wall that is 5.65 m high. Figures 7 and 8 show the collected and the simulated values obtained in this situation, for a satellite with an elevation decreasing from 13 degrees to below the mask angle.

Figure 6 shows all the second order interaction rays that the simulator could determine for that situation. We see that the direct ray is combined with several rays. Among those, are a ray

reflected by the ground, a ray reflected by the building wall, a ray reflected by the ground and by the wall, plus diffracted rays.

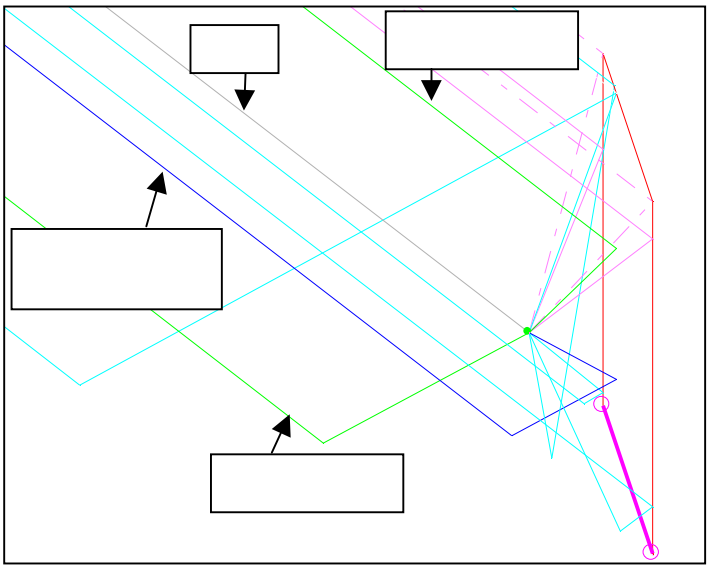

Figure 6: *Result of the ray tracing operation performed by the simulator.*

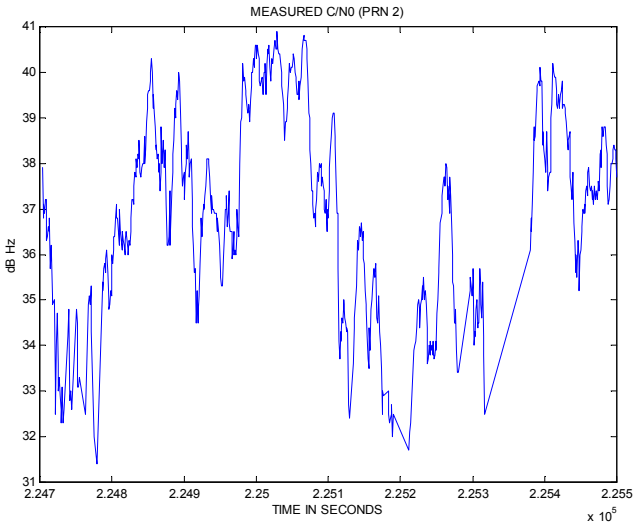

Figure 7: *Measured C/N0 for a patch antenna 2.15 m above the ground and close to a building.*

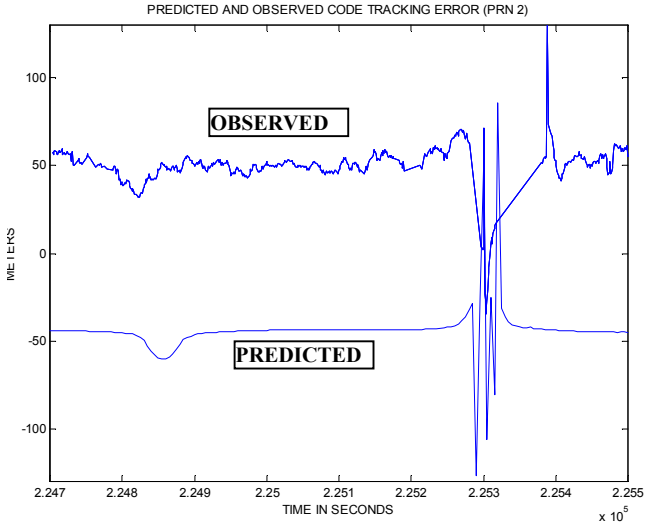

Figure 8: *Comparison of predicted and observed code tracking error for a patch antenna 2.15 m above the ground and close to a building.*

Figure 7 shows the elevation and the measured C/N_0 for PRN 2. As we can see, the measured C/N_0 shows that the signal is disturbed in a different way than in the previous cases, as we can see by comparing figures 2 and 7. The C/N_0 even goes down under the tracking threshold, causing the loops to lose lock several times during this interval. Clearly, there are more than one reflected ray entering the tracking loops.

The upper part of figure 8 shows the extracted code tracking error using the technique presented in section II. As we can see, the error is much larger than in the previous case, and the final part shows that the loops have lost track of the signal for a moment. As in the previous case, the curve has a high frequency component due to the noise, and a low frequency component that has large variations which is attributed to multipath.

The lower part of figure 8 shows the code tracking error that is predicted using the simulator. We can see that the predicted tracking error has the same large scale variations as the observed error, with a slight delay in time. In particular, the predicted error drops down by about 10 meters in the beginning, and it is erratic at the end, just like the observed error. This kind of result could only be achieved by taking into account the two major obstacles interacting with the signal, namely the Earth's surface and the building wall. However, smaller variations of the low frequency component visible on the upper plot of figure 8 could not be reproduced, and may be attributed to other obstacles that were not modeled.

IV. CONCLUSION

The siting tool presented in this paper is composed of a simulator and a measuring tool.

The simulator has undergone a theoretical and practical validation process which is about to be finished. The first results of this validation process showed that the simulator could predict the code tracking error with a satisfying accuracy when only simple obstacles are involved, such as the ground and buildings. These results also confirmed that the simulator can not precisely predict the tracking errors when the environment can not be modeled with a sufficient accuracy.

ACKNOWLEDGMENTS

The authors wish to thank the STNA for supporting this research, and SEXTANT AVIONIQUE for having provided technical assistance.

REFERENCES

Braasch M. (1994) *« Isolation of GPS Multipath and Receiver Cracking Errors »*, in proceedings of ION National Technical Meeting, San Diego, January 24-26.

Braasch M. (1996) *« Global Positioning System: Theory and Applications »*, volume 1, chapter 'Multipath Effects', pages 547-568, AIAA.

Macabiau C., Roturier B., Benhallam A. and Renard A. (1998) *"Development of an end-to-end GPS simulator as a tool for siting GPS reference stations on airport platforms"*, proceedings of ION GPS 98, Nashville, September 15-18.

Macabiau C., Roturier B., Chatre E. and Renard A. (1999) *"Airport multipath simulation for siting DGPS reference stations"*, proceedings of ION National Technical Meeting, San Diego, January 25-27.